

---

## **STREAM SEDIMENTS SURVEY FOR URANIUM IN WADI**

### **EL-REDDAH, NORTH EASTERN DESERT, EGYPT**

**EL NAHAS, H. A., DESOUKY, O. A., ABDEL MONSIF, M., ELSAYED, N. S.**

---

*Nuclear Materials Authority (NMA), P.O. Box 530 El Maadi, Cairo, Egypt*

---

#### **ABSTRACT**

*The radiometrical study carried out for the stream sediments of Wadi El-Reddah reveals that uranium is in a disequilibrium state and uranium concentrations in recent uranium deposits are seldom detected by scintillometer. On this base, two types of uranium deposits of the studied sediments are recorded; old and recent uranium deposits.  $eTh/eU$  ratio of old uranium deposits in the studied sediments suggests poor weathering and rapid deposition of rock detritus. On the other hand,  $eTh/eU$  ratio of recent uranium deposits indicates that these sediments are developed under conditions where uranium was removed from its source and fixed in the sediments with continuous recharge. Two notifications were recorded, the first concerning with the stable increasing of uranium in all directions of Wadi El-Reddah and uniformly decrease in the central part. The second related to the uniform vertical distribution of uranium to one meter depth and may become different in more depths. The qualitative and quantitative mineralogical studies on the stream sediments of Wadi El-Reddah reveals that the most important heavy minerals include uranotorite, zircon, monazite, xenotime, apatite and cassiterite as well as opaque minerals such as ilmenite, magnetite, rutile and hematite. Some very rare minerals were observed in the stream sediments as bismite.*

*Alpha spectrometry plays an important role in the determination of uranium isotopes concentration in the recent samples. The extraction for uranium was increased after modification of the old radiochemical procedure.*

#### **I. INTRODUCTION**

Wadi El Reddah area is delineated by longitudes  $33^{\circ} 20'$  and  $33^{\circ} 22' 30''$ E and latitudes  $27^{\circ} 06' 15''$  and  $27^{\circ} 08' 30''$ N. Wadi El-Reddah is mainly trending N-S and filled with stream sediments. The main outcrops in the study area are older granitoids, Hammamat sedimentary rocks, Monzogranite, Alkali feldspar granites, Post-granite dykes and stream sediments (Fig.1).

Terrestrial radionuclides from the uranium and thorium decay series, commonly associated in nature, are a natural source of radiation. The uranium and thorium decay series together with soil  $^{40}\text{K}$  concentrations, make the major contribution to the total terrestrial gamma flux. Radionuclides in soils occur in minerals or are adsorbed onto soil colloidal components (organic matter, clays, Fe-Mn oxides). From an environmental point of view, processes acting on their transfer and bioavailability are an important issue. The distribution of natural radioisotopes in soil depth profiles has been studied by several authors (e.g. Rosholt et al., 1966; Sully et al., 1987). The effects of soil properties in biogeochemical mobilization of these radionuclides has been gained in recent years e.g. by de Jong et al., (1994). Cowart and Burnett (1994) indicated that  $^{238}\text{U}$  may form complex ions and migrate downward in the

soil profile. The increase of pH with depth may favor leaching of uranyl complexes downward the soil profiles and their further binding to finer soil particles at deeper layers where they are more abundant. This would agree with findings of other authors which indicate radioactivity increase with decrease of particle size (Megumi et al., 1982; Baeza et al., 1995; Navas et al., 2002).

Radioactive uranium and thorium content, from 4.1 to 25.2 ppm and from 12.5 to 30.2 ppm respectively, are recorded by Remon et al., (2006). The stream sediments of Wadi El-Reddah were also studied by El Nahas et al., (2011) using remote sensing and GIS techniques, and recorded U contents ranging from 187-440 ppm.

This work aims at undertaking radiochemical and mineral exploration of the investigated sediments to reveal points of evidences of recent uranium accumulations properly U dispersing aureoles in these sediments.

#### **II. Analytical Techniques**

Stream sediments have filled most of the study area which located at the northeastern part of G. Gattar. Wadi El Reddah is considered as a semi-closed drainage, which allows the various elements to sink within the wadi rather than to be transported over long distances away from

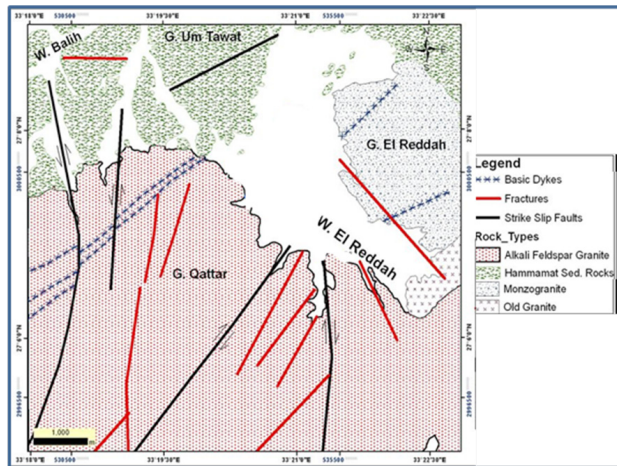


**Fig. 1: Geological map of Wadi El-Reddah area.**

their source rocks. These sediments are mainly composed of loose sands mixed with gravels, pebbles and rarely cobble.

Thirty five trenches were drilled on a grid pattern manner. The trenches are about 300m apart in the same profile. Actually, the collected samples from the drilled trenches were classified into two groups. The first ones collected from the upper 50cm, while the second are from 50 to 100cm depth. Each samples weighed about 3Kg. the samples were quartered using John's splitter and an automatic rotary splitter to obtain representative samples for radiometrical, radiochemical and mineralogical analyses.

The uranium contents were measured radiometrically in the studied stream sediments using NaI-detector, chemically by Spectrophotometric Analysis and radiochemically by Alpha Spectrometer. Also, a representative sample was measured by HPGe-detector. A total 59 samples were measured radiometrically.

### **II.1 NaI and HPGe- detectors**

Uranium, thorium and radium contents were determined by a Bicorn Scintillation Detector NaI (Tl) 76x76 mm with a multichannel analyzer. The collected samples were crushed to about 1 mm grain size, and then packed in plastic containers, sealed and stored for at least 21 days to accumulate radon in order to attain radioactive equilibrium and be ready for the radiometric measurements. Calibration of Na-I detector was carried out by using gamma emitting sources Co-57 (122.1 kV, set up in channel 122) and Cs-137 (661.6 kV, set up in channel 662) as follows:

a- Calibration starts with the Cs-137 source (coarse adjustment) and then with Co-57 source (fine adjustment).

b- The Cs-137 source is repeatedly used as minimum procedure.

c- Since the electrical noise of the photomultiplier in the detector unit generates low amplitude pulses, the lower level discrimination of the instrument must be set up to the level of channel 40 in order to avoid such pulses as well as natural cosmic and X-rays from the registered signals.

The samples were measured through the system and then related to the standards for U, Th, Ra, and K provided by the International Atomic Energy Agency (IAEA). The samples were measured two times 1000 second per each, and then the average of the total counts for each sample was taken. These counts are input to a computer program (analysis) written using Pascal language (Matolin, 1990) which run under MS-Dos to calculate the concentrations of the radioelements (U, Th & Ra in ppm) and K (in %).

Only one sample was analyzed, using gamma-ray spectrometry with HPGe detector. The detector has a relative efficiency of about 50% of the 3" x 3" NaI (Tl) crystal efficiency, resolution of 1.90 keV and peak/Compton ratio of 69.9:1 at the 1.33 MeV gamma transition of <sup>60</sup>Co, then coupled to conventional electronics, connected to a multichannel analyzer card (MCA) installed in a PC computer. The detector was shielded from the background radiation using a 10 cm thick lead, internally lined with a 2 mm copper foil. The software program MAESTRO-32 was used to accumulate and analyze the data. The system was calibrated for energy to display gamma photo peaks between 63 and 3000 keV. The efficiency calibration was performed by using three well-known reference materials obtained from the International Atomic Energy Agency for U, Th and K activity measurements: RGU-1, RGTh-1 and RGK-1 (IAEA, 1987; Anjos et al., 2005).

### **II.2 Alpha procedure**

Several steps of sample preparation, radiochemical separation, and source preparation were performed before analysis. The concerned

sample was leached by mixture of acids in presence of hydrogen peroxide then ashed and spiked with uranium tracer ( $^{232}\text{U}$ ) for chemical yield and activity calculation. Then uranium was extracted from the matrix elements with trioctylphosphine oxide (TOPO) and Di-2-ethylhexylphosphoric acid (D2EHPA) and stripped with 0.75M  $\text{Na}_2\text{CO}_3$  solution. Modifications were performed for the procedure to give highest extraction. The uranium fraction was purified by co-precipitation with  $\text{LaF}_3$  to ensure complete removal of thorium and traces of resolution degrading elements. This was followed by a final clean-up step using an anion exchange. The pure uranium fraction was electrodeposited on a stainless steel disc from HCl/oxalate solution.

### ***II.3 Spectroscopy procedure***

Uranium (VI) using Arsenazo (III) was determined by the spectrophotometer apparatus which is "Metertech Inc" model SP-8001, UV-Visible spectrophotometer. This apparatus is a single beam recording spectrophotometer and covers the UV-Visible range 200-1100 nm with wavelength accuracy of  $\pm 1\text{nm}$ . One match of 5 cm<sup>3</sup> quartz cell with a path length of 1cm was used for both samples and blank reagent. All measurements were carried out in Nuclear Materials Authority Labs in which a small portion of the sample (0.25ml) is added to 1.5 ml of 0.25% Arsenazo III and after that add 2 ml of  $\text{NH}_4\text{OH}$  and shaking for 3 min. and after a few minutes, add 4 ml of Urea nitric and up to volume with distilled water in 10 ml volumetric flask and left for 15 min. and then measure the sample on Spectrophotometer (Marchzenko, 1986).

## **III. RESULTS AND DISCUSSION**

### ***III.1 Distribution of uranium and thorium***

The obtained data resulted from the radiometric, chemical and radiochemical analyses for the studied samples are listed in Table (1) and represented in figure (2). The data show wide variation in U, Th, Ra (eU) and K% contents; U up to 17 ppm, and Th up to 43 ppm. Ra(eU) varying between 5 and 17 ppm and averaging 8.58 ppm. The content of potassium falls between 2.34 ppm and 5.31ppm with an average of 3.42 ppm.

The data of the studied sediments are compared with the averages of arenaceous and argillaceous sediments (Table 1) reported by IAEA (1979) and Boyle (1982). It is clear that these samples have higher contents of uranium and thorium than the arenaceous sediments and also the average of greywacke reported by Killen (1979). Average of uranium contents are higher than argillaceous sediments while average of thorium values fall within the range of argillaceous sediments. Th/U ratio average (2.57 ppm) is slightly lower than average of arenaceous and argillaceous sediments.

It is important to mention that, there is a clear difference between chemically, radiochemically and radiometrically uranium contents (Table 1). This is resulted from the fact that when uranium is too recently deposited, it is difficult to build up radioactive daughter products. So, uranium concentrations are seldom detectable by scintillometer. On this base, two types of uranium deposits are recorded, old and recent uranium deposits.

The U-contents and Th/U ratios in sedimentary rocks are generally used to deduce the conditions under which the highly anomalous mineralized or uraniferous types were formed (Adams and Weaver, 1958). However, three types of sediments are differentiated according to their Th/U ratios:

i. The first type includes sediments of Th/U ratio value ranging between 0.012- 0.81. These sediments are developed under conditions where uranium was removed from its source and fixed in the sediments with continuous recharge.

ii. The second type of sediments has Th/U ratio value ranging between 1.47-1.49. They are characterized by their relatively high Th-content, regarding to the first one, due to slightly more scavenging of U-content because of continuous leaching and recharging.

iii. The third type of sediments, exhibits Th/U ratio value ranging between 1.49 & 5.47. These sediments reflect the poor weathering and rapid deposition of rock detritus. Therefore, the detrital radioactive minerals like xenotime, samarskite, thorite and euxenite usually dominate in this type.

**Table (1): Radiometric measurements of eU, eTh, Ra (eU) and K% and chemical analysis of uranium (U) for the studied stream sediments of Wadi El-Reddah.**

Samples no.		eU (ppm)	eTh (ppm)	Ra(eU) (ppm)	K %	eTh/eU	eU/Ra	Uc	Uc/Ur
D/0	U	10	16	5	2.44	1.60	2.00		
	B	11	20	5	2.71	1.82	2.20		
D/300E	U	12	21	6	2.99	1.75	2.00		
	B	7	16	5	2.96	2.29	1.40		
J/0	U	13	16	7	3.79	1.23	1.86	479.60	36.89
J/300W	U	10	23	8	3.66	2.30	1.25		
P/0	U	6	20	6	2.83	3.33	1.00		
	B	9	20	6	2.65	2.22	1.50		
P/300E	B	6	17	6	2.98	2.83	1.00		
P/600E	U	6	16	5	3.76	2.67	1.20		
P/300W	U	6	20	7	4.04	3.33	0.86		
	B	16	26	9	3.80	1.63	1.78		
S/300E	U	5	19	8	3.75	3.80	0.63	400.65	80.13
	B	6	17	7	3.60	2.83	0.86	408.60	68.10
S/600E	U	11	20	5	4.28	1.82	2.20	353.15	32.10
	B	4	18	5	4.28	4.50	0.80	407.15	101.79
S/300W	U	8	21	9	4.00	2.63	0.89	153.90	19.24
	B	7	22	9	3.69	3.14	0.78	366.80	52.40
S/600W	U	11	20	9	4.24	1.82	1.22	309.80	28.16
	B	9	24	8	3.44	2.67	1.13	264.65	29.41
V/900W	B	9	27	11	3.13	3.00	0.82		
Y/0	U	16	28	8	2.58	1.75	2.00		
	B	8	15	7	3.63	1.88	1.14		
Y/300E	B	8	19	8	3.04	2.38	1.00		
Y/600E	U	11	30	8	3.51	2.73	1.38		
	B	11	18	7	2.75	1.64	1.57		
Y/300W	U	16	28	9	4.71	1.75	1.78		
	B	5	19	9	3.56	3.80	0.56		
Y/600W	U	5	21	7	2.99	4.20	0.71		
	B	9	22	9	3.45	2.44	1.00		
DD/0	U	14	23	11	4.24	1.64	1.27		
	B	10	17	7	3.82	1.70	1.43		
DD/300E	B	13	26	8	3.05	2.00	1.63		
DD/600E	U	13	29	11	3.03	2.23	1.18		
DD/900E	B	10	16	7	3.08	1.60	1.43		
DD/300W	B	13	22	6	2.62	1.69	2.17		
	B	13	22	15	3.09	1.69	0.87		
GG/0	U	12	29	8	4.08	2.42	1.50	288.60	24.05
	B	7	30	10	3.54	4.29	0.70	454.95	64.99
GG/300E	U	7	23	11	4.10	3.29	0.64	199.05	28.44
	B	5	33	17	5.29	6.60	0.29	534.30	106.86
GG/600E	U	17	27	10	2.69	1.59	1.70	151.35	8.90
	(B)	12	24	10	3.70	2.00	1.20	480.35	40.03
GG/900E	(U)	9	22	9	2.34	2.44	1.00	547.25	60.81
	B	9	29	11	3.55	3.22	0.82	274.15	30.46
GG/300W	U	15	25	7	2.46	1.67	2.14		
	B	11	21	7	2.42	1.91	1.57		
GG/600W	U	6	32	9	2.89	5.33	0.67		
	B	9	28	9	3.01	3.11	1.00		
JJ/0	U	17	34	13	3.03	2.00	1.31		
	B	5	25	12	3.54	5.00	0.42	153.30	30.66
JJ/300E	U	10	28	11	3.96	2.80	0.91	425.45	42.55
	B	11	27	11	3.74	2.46	1.00	439.00	39.91
JJ/600E	U	11	27	10	3.38	2.46	1.10	600.00	54.55
	B	12	25	14	5.31	2.08	0.86	792.40	66.03

Sample no.		eU (ppm)	eTh (ppm)	Ra(eU) (ppm)	K %	eTh/eU	eU/Ra	Uc	Uc/Ur
JJ/900E	U	9	31	10	3.50	3.44	0.90	446.80	49.64
	B	12	27	8	3.62	2.25	1.50	287.50	23.96
MM/600E	B	15	20	7	2.73	1.33	2.14		
	U	16	43	12	3.58	2.69	1.33		
MM/900E	B	13	23	6	2.80	1.77	2.17		
	U	16	43	12	3.58	2.69	1.33		
Min.		4	15	5	2.34	1.23	0.29	151.35	8.90
Max.		17	43	17	5.31	6.60	2.20	792.40	106.86
average		10.12	23.50	8.58	3.42	2.57	1.26	384.11	46.67
*ArenaceousS		1	3	-	1.4	3	-	-	-
**Argillaceous		4	16-47	-	2.7	4	-	-	-
*** greywacke		1.5	5	-	-	-	-	-	-

\* Arenaceous sediments (IAEA, 1979 and Boyl, 1982)

\*\* Argillaceous sediments (IAEA, 1979 and Boyl, 1982)

\*\*\* Average of greywacke (Killen, 1979)

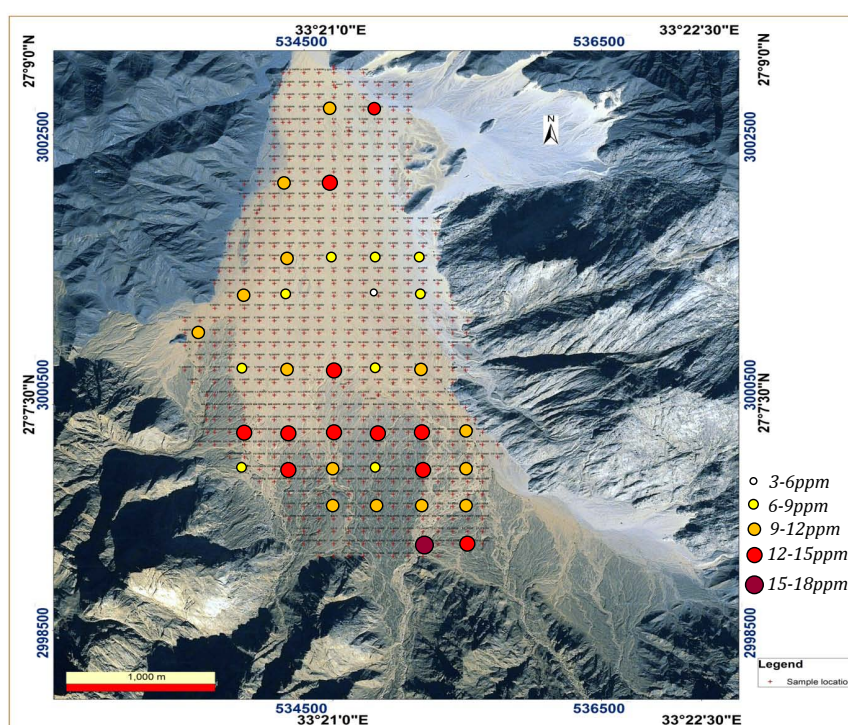


Fig. (2): Distribution of radiometrically U content in the studied stream sediments

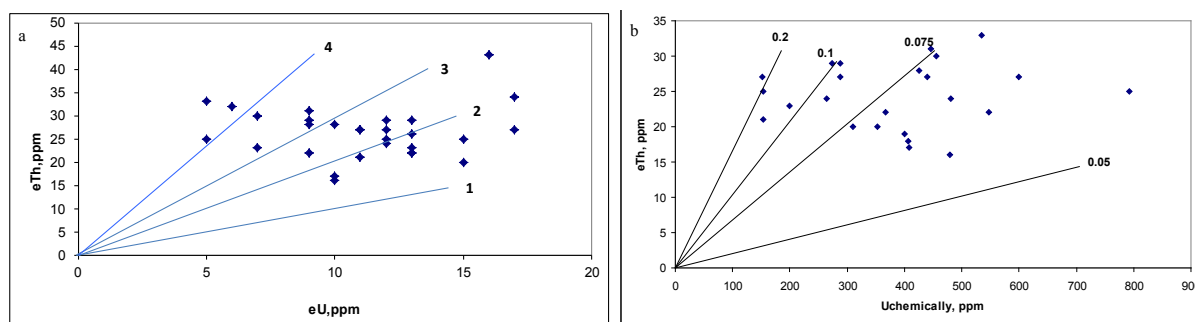


Fig. (3): a) eTh-eU variation diagram, b) eTh-U<sub>c</sub> variation diagram

The obtained data indicates that the  $eTh/eU$  ratio values of old uranium deposits of the studied sediments lie in third group where the poor weathering and rapid deposition of rock detritus are dominated (Fig.3a).

On the other hand, recent uranium deposits of the studied sediments in the first group, indicating that these sediments are developed under conditions where uranium was removed from its source and fixed in the sediments with continuous recharge (Fig. 3b).

### III.2 Radioactive equilibrium

According to Reeves and Brooks (1978), uranium ( $U^{238}$  series) attains the equilibrium state in nearly 1.5 M.a. Cathelineau and Holliger (1987) stated that uranium mineralization is affected by different processes. Leaching, mobility and redistribution of uranium are affected by hydrothermal solutions and/or supergene fluids, which cause disequilibrium in the radioactive decay series in the U-bearing rocks. The radioactive equilibrium of the studied sediments can be determined by the calculation of equilibrium factor (P) which is the ratio of radiometric uranium contents (eU) to the radium content Ra(eU);  $P_{factor} = eU/Ra(eU)$  (Hussein, 1978; El-Galy, 1998; Surour et al., 2001; El-Feky et al., 2011). The average ratio of  $P_{factor}$  of the studied sediments is 1.26 which is more than one. Figure (4a) indicates disequilibrium in U-decay series due to uranium addition.

The second method for the study of equilibrium is carried out by using the data of chemically analyzed uranium ( $U_c$ ) and radiometrically determined uranium ( $U_r$ ). Ratio between chemically and radiometrically determined uranium is known as the D-factor =  $U_c/U_r$  (Hansink, 1976). Another factor controlling the equilibrium state is the loss of radon gas as one of uranium daughters. This loss occurs easily due to the solubility of radon in water and its leakage through pore spaces as well as along faults and other fractures types. The use of D-factor in the determination of equilibrium state of the studied sediments reveals that the studied sediments have chemically analyzed uranium greater than the radiometrically determined uranium reflecting a disequilibrium state characterized by addition of uranium (Fig. 4b).

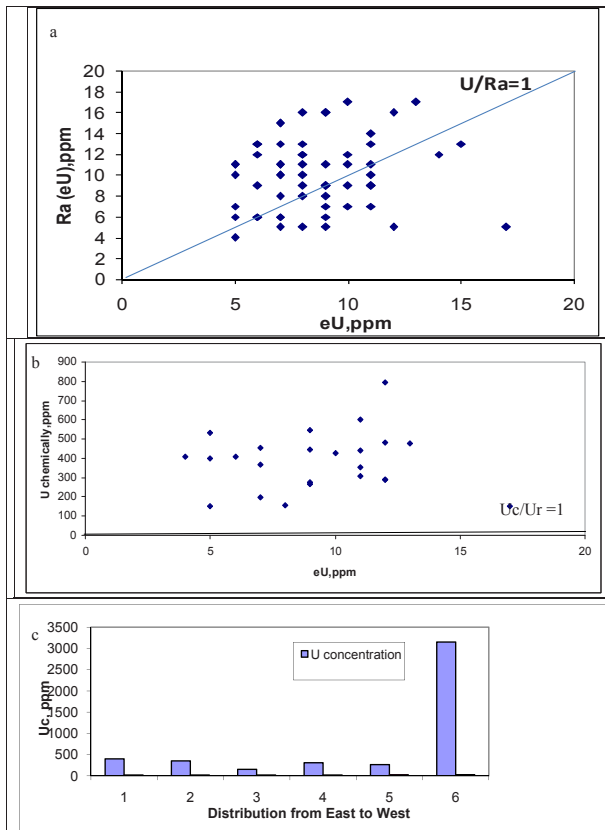


Fig. (4): a) Ra-eU variation diagram, b)  $U_c$ -eU variation diagram and c) E-W uranium distribution diagram

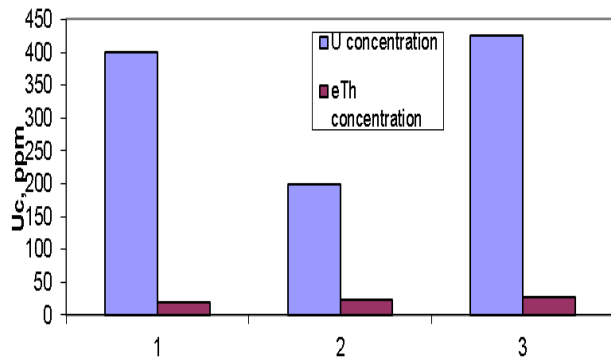


Fig. (5): N-S uranium distribution diagram

rium state characterized by addition of uranium (Fig. 4b).

### II.3 Source of uranium accumulations

For determination of the source of anomalous uranium aureoles in the studied stream sediments, two traverses will be carried out for following of radioelement distribution. The first transection takes the E-W direction which the second has the N-S direction (Fig.4c and Fig.5). In the E-W, radioactivity is very high in the west and slightly high in the east indicating the uptake

from the two directions and the source is mainly from G. Gattar in the west direction and G. El-Reddah in the East direction (Fig.4c). On the other hand, the radioactivity increases in the north and south directions suggesting uranium mobilization from the same previously mentioned peaks. Anomalous uranium contents could be attributed to the presence new anomalous occurrences in the altered portions of G. Gattar and G. El-Reddah which decant in these directions. Also, two notifications were recorded, the first concerning with the stable increasing of uranium in all directions of W. El-Reddah and uniformly decrease to the central part. The second related to the uniform vertical distribution of uranium to one meter depth.

Notable decreasing in  $^{234}\text{U}/^{238}\text{U}$  ratios from decants to the central parts (Table 2) could have been produced if recent U enrichment was superimposed on an earlier U which had either produced no  $^{234}\text{U}/^{238}\text{U}$  disequilibrium or had diminished disequilibrium through decay (Prikrýl et al., 1997).  $^{234}\text{U}/^{238}\text{U}$  activity ratios in excess of 1 (sample DD/300W) suggest that U was mobilized and transported away from the primary deposit within the last 1 Ma. Although  $^{234}\text{U}$  and  $^{238}\text{U}$  have similar chemical behavior and should therefore not be fractionated by chemical weathering of minerals, several authors have shown that this assumption is not verified in nature. The reason why  $^{234}\text{U}/^{238}\text{U}$  activity ratios of weathered solids are lower than unity is known as the  $\alpha$ -recoil effect and is explained by the preferential leaching of  $^{234}\text{U}$  from  $\alpha$ -recoil-damaged lattice sites in minerals. Conversely, the solid phase is enriched in  $^{238}\text{U}$  (Brantley et al., 2008). In most stream sediment samples,  $^{234}\text{U}/^{238}\text{U}$  ratio is low (0.42), suggesting  $^{238}\text{U}$  was enriched at the expense of  $^{234}\text{U}$ , the later may be leached and migrated to higher depths or to the underlying groundwater.

**Table (2): Uranium concentration in Wadi El-Reddah samples measured by HPGe-detector and Alpha spectrometry**

Method of analysis	Sample no.	$^{238}\text{U}$ (Bq/Kg)	$^{234}\text{U}$ (Bq/Kg)	$^{235}\text{U}$ (Bq/Kg)	$^{234}\text{U}/^{238}\text{U}$
Alpha spectrometry	JJ/600E(U)	11000.00	4621.80	-	0.420
	S/300E (U)	7557.00	6058.60	-	0.801
	V/900W	39064.30	15087.70	-	0.386
	DD/300W	35402.30	38850.27	-	1.097
HPGe- detector	JJ/600E(U)	1966.68	1908.02	85.22	0.970

#### IV. Mineralogy

##### IV.1 Heavy Minerals Study

Thirty six stream sediment samples were collected in grid pattern manner from the upper 50cm of the stream sediments of W. El Reddah to investigate qualitative mineralogical analysis of these deposits. These samples were grouped in three composite samples representing the whole area of W. El-Reddah. Each sample was sieved using 2mm sieve to remove trash from the sample, the samples was subjected to gravity separation process using a wiffey shaking tables. The obtained fractions resulted from the separation using shaking tables are concentrate, middling and a rejected tailing. The concentrates of the composite samples were dried and prepared for the heavy liquid separation using bromoform solution (Sp.gr.  $\sim 2.81\text{g}/\text{cm}^3$ ). The heavy fractions resulted from the heavy liquid separation are clustered in the size fractions between 1mm and 0.063mm. The heavy fractions obtained from bromoform separation were subjected to another heavy liquid separation using methylene iodide (diiodomethan, Sp.gr.  $\sim 3.32\text{g}/\text{cm}^3$ ). The heavy fractions resulted from the separation by methylene iodide were subjected to magnetic separation using a permanent magnet, to separate magnetite, and Frantz Isodynamic Magnetic Separator (Model L1) at 0.2, 0.5 current ampere to differentiate the considered minerals in magnetic subfractions. The subfractions obtained by magnetic separation were carefully examined using Binocular Stereomicroscope. The identification of the different minerals in the studied stream sediments of Wadi El Reddah area was carried out by using X-ray diffraction technique (XRD) and a Philips Environmental Scanning Electron Microscope (ESEM) model XL30. The percentage of heavy minerals, separated by bromoform solution have an averages 3.9% whereas

the percentages of heavy minerals resulted from separation by methylene iodide solution have an average of 1.4%. It is worthy to point out that the light fractions of all samples contain abundant quartz, feldspar and micas contributed from the granite. The heavy minerals are more concentrated near the foot of G. Gattar. This may be due to the sedimentological conditions controlling the deposition of these minerals as the light gangue mineral can move to the middle parts of the wadi. A strong positive relation between the percentages of heavy minerals separated by bromoform and that separated by methylene iodide ( $r = 0.8$ ) was noticed. The magnetic fractionation of the heavy minerals was carried out to facilitate the process of the counting of these minerals under the binocular microscope. The heavy minerals are mainly clustered in the magnetic fraction separated at 0.2 ampere followed by the magnetic fraction separated at 0.5ampere, whereas the lowest concentration of the heavy minerals is recorded in the nonmagnetic fractions. The most important heavy minerals in the studied stream sediments of W. El Reddah include uranothorite, zircon, monazite, xenotime, apatite and cassiterite as well as opaque minerals such as ilmenite, magnetite, rutile and hematite. Some very rare minerals were observed in the stream sediments as bismite.

**Uranothorite [ $\text{ThU}_2\text{SiO}_7$ ]:** Uranothorite in the studied stream sediments of Wadi El-Reddah exhibits subhedral, rarely euhedral and medium to fine opaque grains. The color of the mineral varied from black to brownish black color with

metallic to submetallic luster (Fig.6a). The EDX mineral analyses of this mineral reflect the composition of uranothorite, where uranium content ranges from 12.42 and 16.38%. The average of Th/U ratio is 3.61, which reflects that thorite mineral grains may be originated from granitic magma with slightly enrichment in U. Some of uranothorite grains contain appreciable amounts of Y and Zr (Fig.6b). The XRD patterns of the studied uranothorite revealed that the growth of its diffraction peaks due to annealing of the mineral and the presence of some hematite diffraction peaks (Fig.7). Uranothorite occurs as a result of the substitution of Th by U, and U may exceed 10% as  $\text{UO}_2$ .

**Zircon [ $\text{ZrSiO}_4$ ]:** Most of zircon grains are medium to fine grains (0.5mm to 0.125mm) and appear as prismatic euhedral to subhedral grains, sometimes with bipyramidal terminations. Rounded, spherical and elongated grains are rarely observed. The majority of zircon mineral grains exhibit intrinsic yellow to yellowish brown color (Fig.8a). The color variation of some zircon grains may be attributed the initial composition of the mineral, metamictizations or inclusions and encrustation by iron oxides. In the studied zircon of Wadi El-Reddah area, it contains appreciable amounts of Hf, Fe, Ca, Al, Mg, U and Th (Fig.8b). Also, the data indicates that there is a preponderance of U over Th, which reveals that the radioactivity of zircon is related to U rather than Th. Zircon-thorite exsolution intergrowths rarely occur in some zircon mineral grains in the form irregular masses of tho-

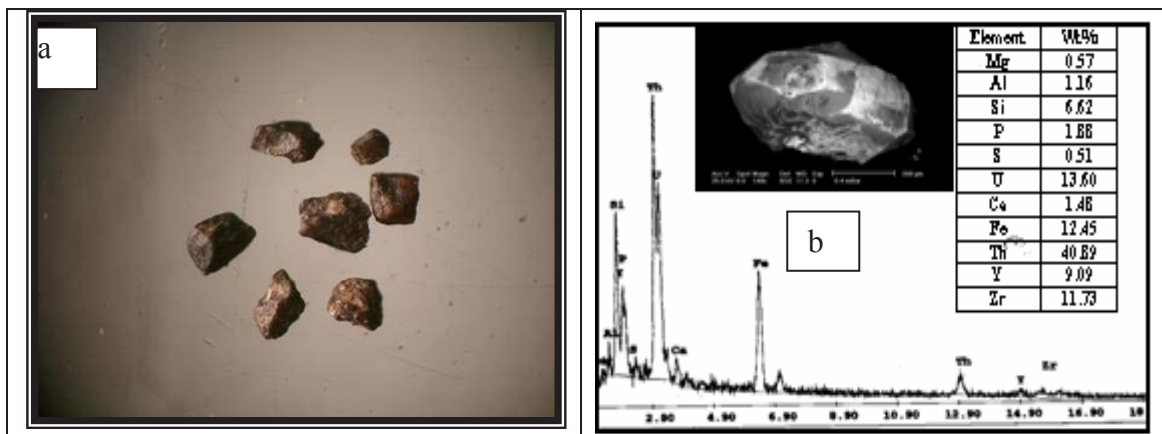


**Fig.6: a) Stereophotomicrograph of uranothorite, b) EDX mineral analysis and BSE image of uranothorite from stream sediments of W. El Reddah.**

rite within zircon crystals (Fig.8c). Some zircon grains contain inclusion of other minerals such as thorite, apatite, silicate minerals and rutile, which confirmed by EDX analyses (Fig.8d).

Monazite [REE P<sub>2</sub>O<sub>5</sub>]: The investigation of monazite mineral grains in the studied stream sediments under the binocular stereomicroscope reveals that the majority of monazite grains display rounded to well rounded, tabular and spherical shapes. They have commonly light canary and lemon yellow color with characteristic resinous luster (Fig.9 a). EDX mineral analyses of some monazite mineral grains indicate that only

four REE; La, Ce, Pr and Nd, represent more than 90% of REE budget of monazite (Fig.9b).

Thalenite-(Y): The general formula of the mineral is (Y<sub>2</sub>Si<sub>2</sub>O<sub>7</sub>). The mineral is very rare in the stream sediments of W. El Reddah, whereas few grains were picked and detected by SEM. It occurs as anhedral tabular elongated to spherical brown to dark brown grains with resinous luster (Fig.10a). SEM analyses of some grains show that they consist mainly of Y, REE and Si. Trace amounts of Ca, Fe, K, U, Th, P and Al (Fig.10b).

Cassiterite [SnO<sub>2</sub>]: Cassiterite is a constituent of highly siliceous igneous rocks, as well as

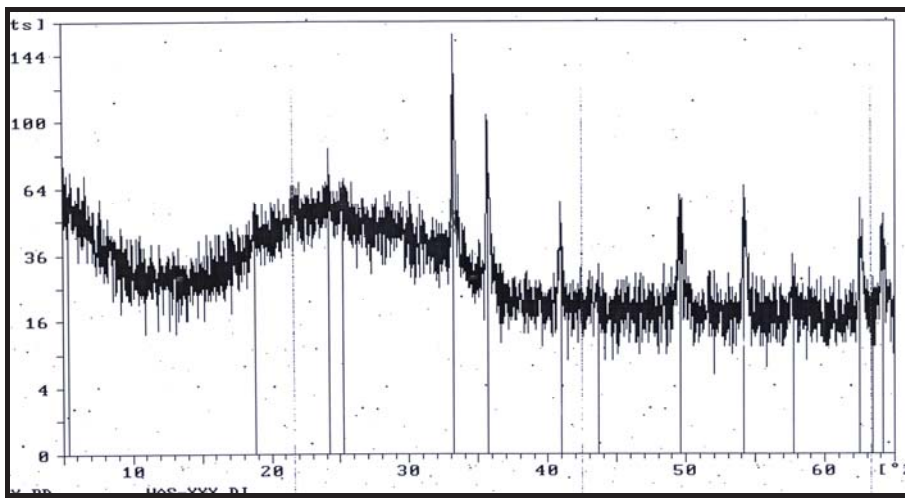


Fig.7: X-ray diffraction pattern of the annealed uranothorite.

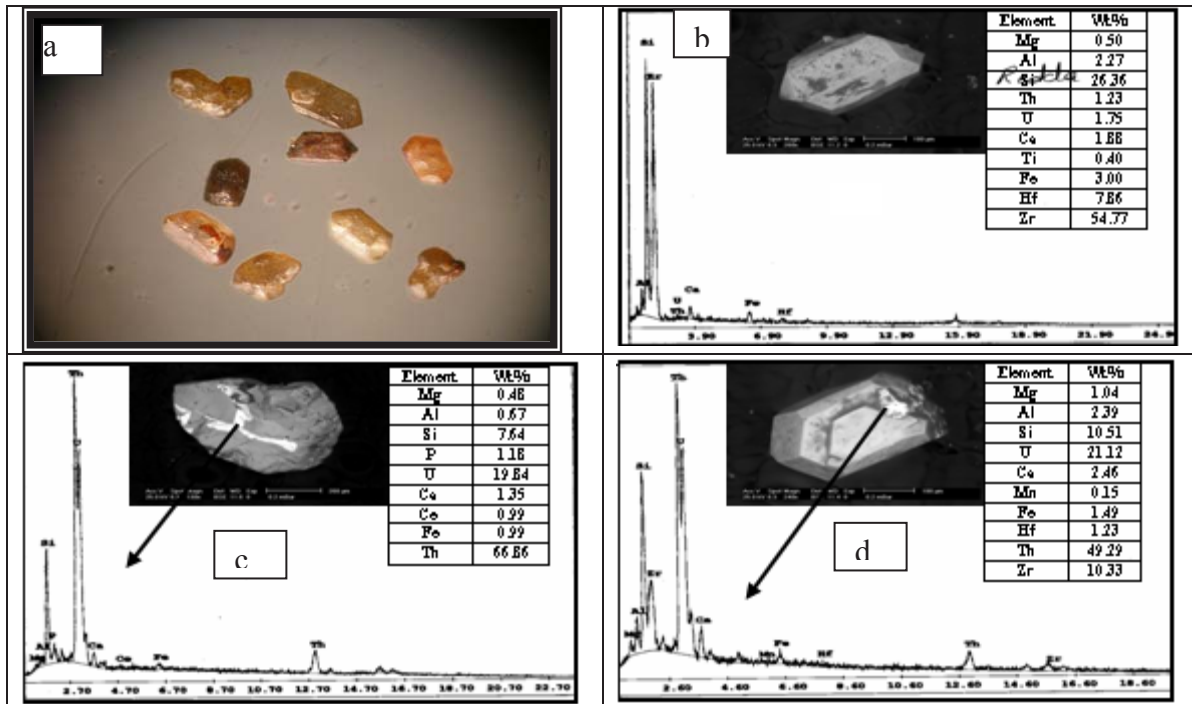


Fig.8: a) Stereophotomicrograph of zircon, (b, c and d) EDX mineral analyses and BSE image of zircon from stream sediments of W. El Reddah.

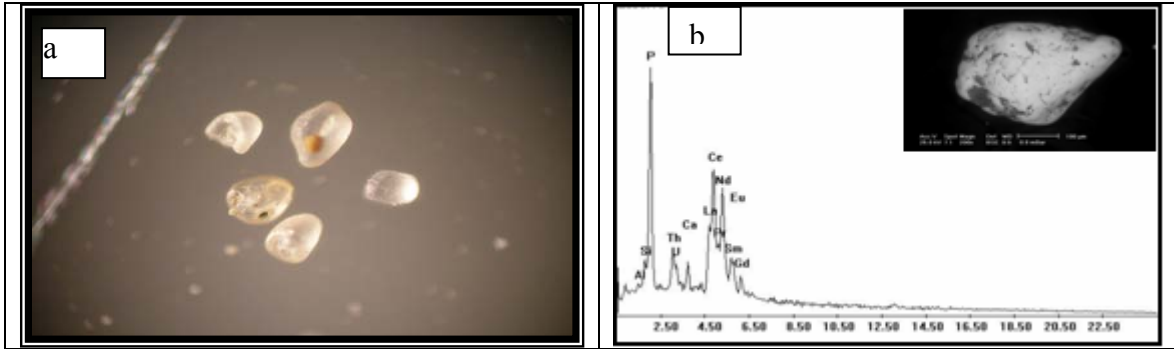


Fig.9: a) Stereophotomicrograph of monazite, b) EDX mineral analyses and BSE image of monazite from stream sediments of W. El Reddah.

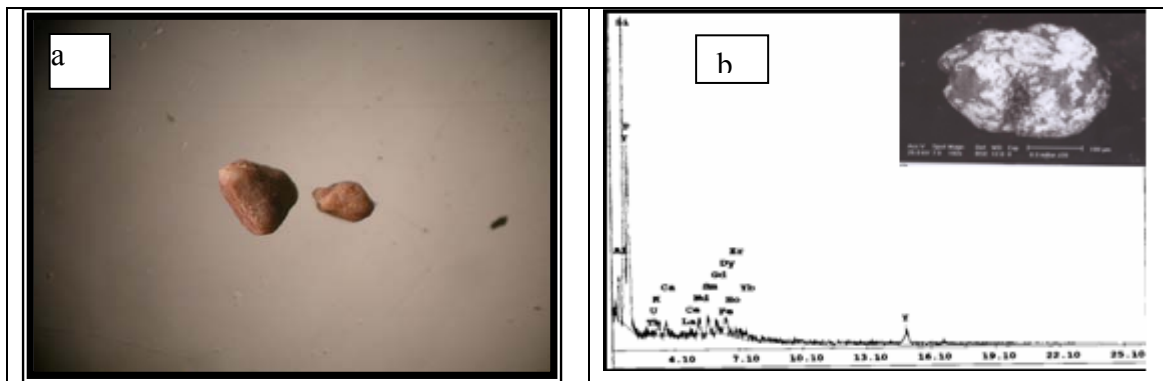


Fig.10: a) Stereophotomicrograph of thalenite, b) EDX mineral analyses and BSE image of thalenite from stream sediments of W. El Reddah.

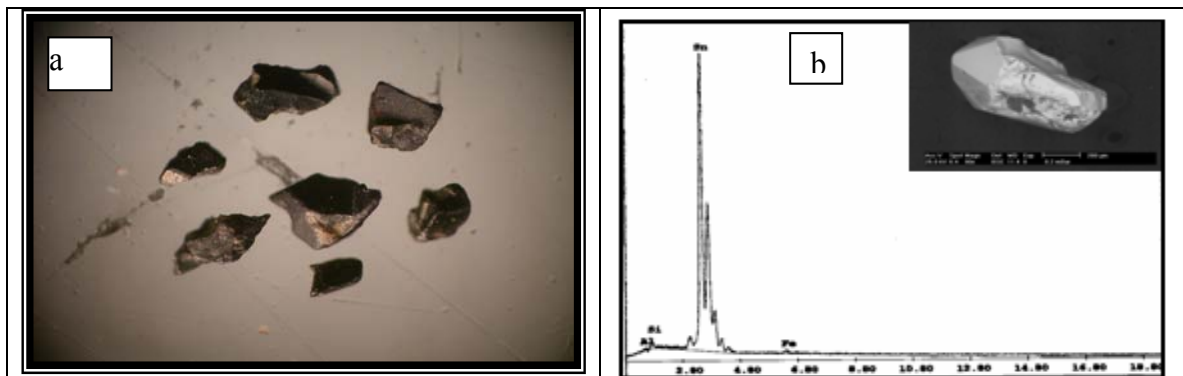


Fig.11: a) Stereophotomicrograph of cassiterite, b) EDX mineral analyses and BSE image of cassiterite from stream sediments of W. El-Reddah.

greisen, granitic pegmatites and in hydrothermal veins. It occurs as euhedral to subhedral crystals and exhibits black to reddish brown colors with adamantine luster. The broken grains are characterized by conchoidal fractures and striae, parallel to principle axis or to pyramidal phases (Fig.11a). It consists mainly of Sn with the presences of trace amounts of Fe, Si and Nb, possibly relating to the intimate association with other elements (Fig.11b). The presence of cassiterite in the stream sediments of W. El Reddah was

confirmed by XRD technique (Table 3).

Apatite: The majority of apatite mineral grains are rounded to well rounded egg-shaped to spherical illustrating the sedimentary origin of these grains. The color of the mineral ranges from smoky white to brownish yellow color (Fig.12a). The SEM analyses of apatite reveal that Ca/P ratio is not stoichiometric due to the weathering effect. Moreover, REEs are not detected in all analyzed apatite grains (Fig.12b).

**Table 3: X-ray diffraction data of cassiterite from the stream sediments of W. El- Reddah.**

Measured values		Cassiterite	
dÅ	I/I <sub>0</sub>	ASTM card (21-1250)	
dÅ	I/I <sub>0</sub>	dÅ	I/I <sub>0</sub>
3.35	100	3.351	100
2.64	94	2.644	81
2.37	45	2.369	24
2.31	7	2.309	5
1.76	80	1.765	63
1.68	16	1.675	17
1.59	6	1.593	8
1.56	18	1.498	13
1.44	7	1.439	17
1.41	21	1.415	15

Associated minerals: these minerals include opaque minerals as hematite, magnetite, rutile and ilmenite. Some very rare minerals were observed in the stream sediments as bismite.

Rutile (TiO<sub>2</sub>): Rutile is a major mineral source of the titanium. Rutile is typically includes about 60% titanium and 40% oxygen. It can have some iron, sometimes up to 10%. Rutile is found in stream sediments of wadi El-Reddah. Its color is blood red, brownish yellow, brown red, violet and black with submetallic luster. It has many shapes as prismatic (Fig. 13a) and elbow (Fig. 13b). Rutile was confirmed by X- ray diffraction (Fig. 14) and ESEM technique and contains (99%) TiO<sub>2</sub> and (1%) SiO<sub>2</sub> (Fig. 14).

Ilmenite (FeTiO<sub>3</sub>): Ilmenite is present as accessory mineral and associated with magnetite in stream sediments of Wadi El-Reddah. Ilmenite can help in fixation of uranium oxide from their uranyl solution as magnetite. Its color is black with metallic to submetallic luster. Ilmenite was confirmed by ESEM technique, and the EDX

analyses give Fe: Ti ratio equal 1:1.1(Fig.16).

Bismite (Bi<sub>2</sub>O<sub>3</sub>): A monoclinic mineral composed of bismuth trioxide, varying in color from green to yellow. Bismite occurs in yellow earth, so it is known as bismuth ocher. With earthy-dull, clay-like texture with no visible crystalline affinity. SEM analyses of some grains show that they consist mainly of Bi. Trace amounts of Ca, Fe and Al (Fig. 17).

### Conclusions

The radiometric measurements of the studied sediments show wide variation in their U, Th, Ra (eU) and K% contents. They show variation of U from 1 to 17 ppm, with an average of 9.85 ppm and Th content between 15 and 43 ppm, with 23.5 ppm as an average. Ra(eU) varying between 5 and 17 ppm and an average of 8.58 ppm. The content of potassium falls between 2.34 ppm and 5.31ppm with an average of 3.42 ppm, while the chemical U range between 151 and 547ppm with an average of .

Based on radiometric and chemical analysis uranium deposits in the studied stream sediments could be classified into: 1- old uranium deposits and 2- young uranium deposits.

The obtained data indicates that the eTh/eU ratio values of old uranium deposits of the studied sediments of poor weathering and rapid deposition of rock detritus. Therefore, the detrital radioactive minerals like xenotime, samarskite, thorite and euxenite usually dominate them.

On the other hand, recent uranium deposits of the studied sediments the first group indicating that these sediments are developed under conditions where uranium was removed from its

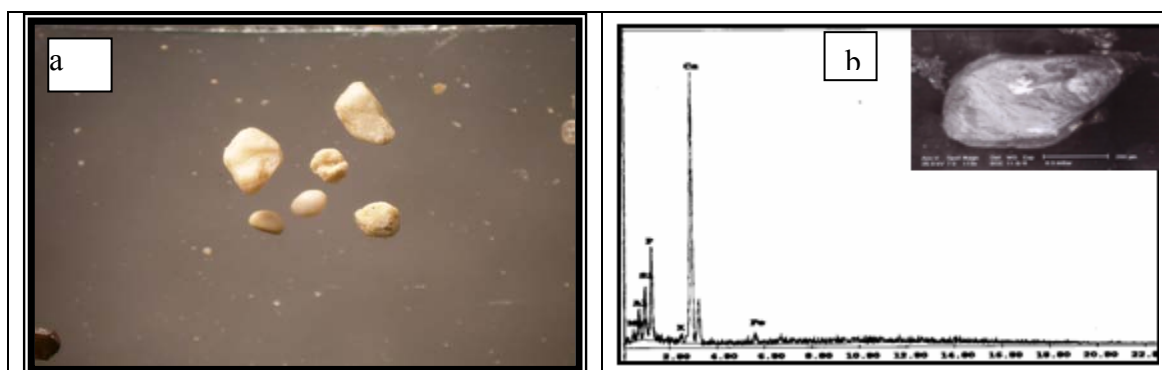
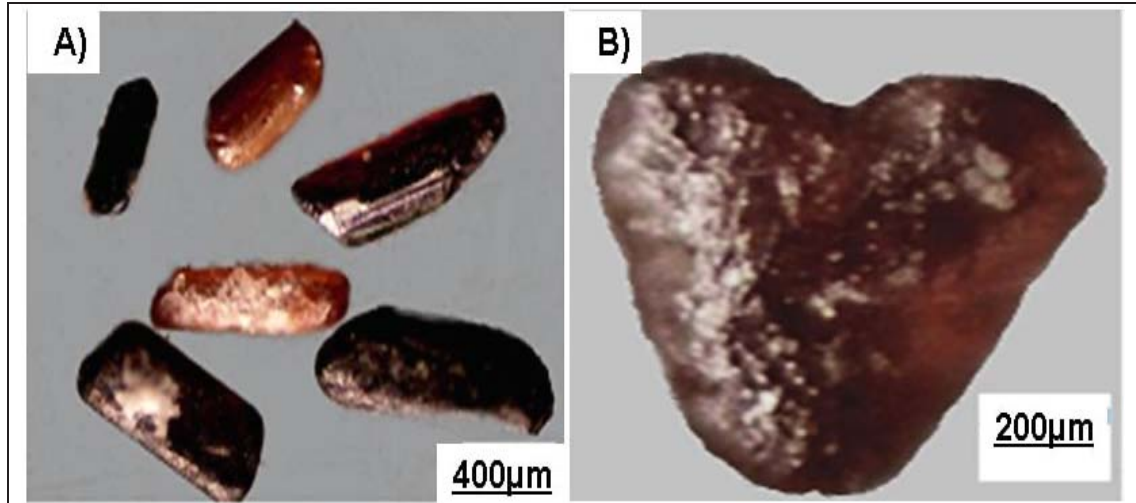


**Fig.12: a) Stereophotomicrographs of apatite, b) EDX mineral analyses and BSE image of apatite from stream sediments of W. El-Reddah.**



Figs. (13): Photographs showing different types of rutile mineral from wadi El-Reddah  
a) Prismatic rutile, b) Elbow rutile.

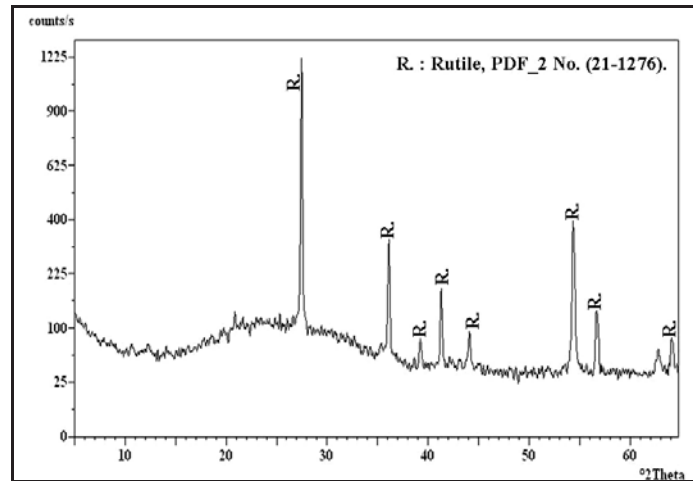


Fig. (14): XRD pattern of rutile mineral from wadi El-Reddah.

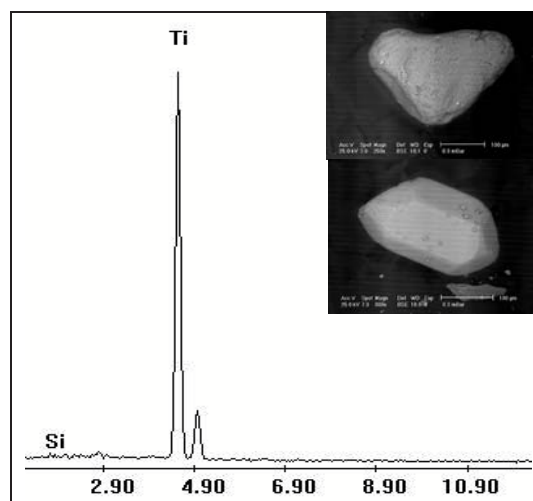


Fig. (15): EDX and BSE image showing rutile mineral from stream sediments of W. El- Reddah.

**Bismite ( $Bi_2O_3$ ):** A monoclinic mineral composed of bismuth trioxide, varying in color from green to yellow. Bismite occurs in yellow earth, so it is known as bismuth ocher.

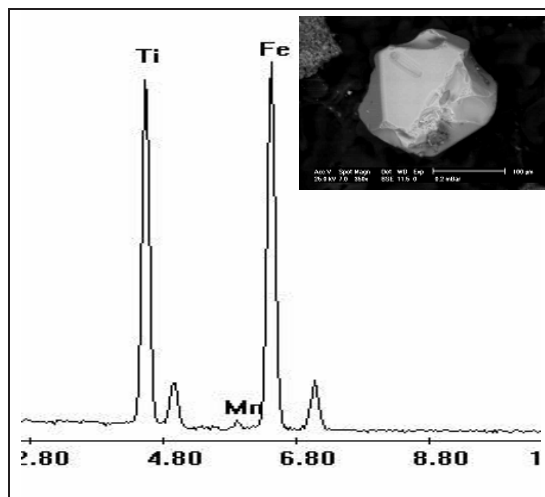


Fig. (16): EDX and BSE image showing ilmenite mineral from stream sediments of W. El-Reddah.

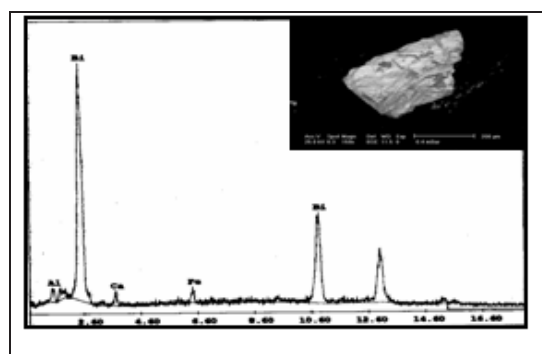


Fig. (17): EDX mineral analysis and BSE image of bismite from stream sediments of Wadi El-Reddah.

source and fixed in the sediments with continuous recharge.

The average ratio of  $P_{\text{factor}}$  of the studied sediments is 1.26 which is more than one indicating disequilibrium in U-decay series due to uranium addition.

The use of D-factor in the determination of equilibrium state of the studied sediments reveals that the studied sediments have in many cases chemically analyzed uranium greater than the radiometrically determined uranium reflecting a disequilibrium state characterized by addition of uranium. In contrast to that, some samples show negative disequilibrium with chemically analyzed uranium less than radiometrically suggesting leaching conditions.

E-W and N-S traverses indicating the distribution of uranium in these directions were studied. In the E-W, radioactivity is very high in the

west and slightly high in the east indicating the uptake of uranium from the two directions and the source is mainly from G. Gattar in the west direction and G. El-Reddah in the east direction. On the other hand, the radioactivity increases in the north and south directions suggesting uranium mobilization from the same previously mentioned peaks. Anomalous uranium contents could be attributed to the presence new anomalous occurrences in the altered portions of G. Gattar and G. El-Reddah which decant in these directions.

The mineral analysis of fourteen stream sediments samples using X-ray diffraction analysis (XRD) and Environmental Scanning Electron Microscopic (ESEM) examination. The analysis revealed that the most important heavy minerals in the studied stream sediments of W. El Reddah include uranothorite, zircon, monazite, xenotime, apatite and cassiterite as well as opaque

minerals such as ilmenite, magnetite, rutile and hematite. Some very rare minerals were observed in the stream sediments as bismite.

## REFERENCES

- Adams, J.A.S., Weaver, C.E., (1958): Thorium to uranium ratios as indications of sedimentary processes: example of concept of geochemical facies: American Association of Petroleum Geologists Bulletin, Vol. 42, pp. 387-430.
- Anjos, R.M., Veiga, R., Soares, T., Santos, A.M.A., Aguiar, J.G., Frasca, M.H.B.O., Brage, J.A.P., Uzêda, D., Mangia, L., Facure, A., Mosquera, B., Carvalho, C., Gomes, P.R.S., 2005. Natural radionuclide distribution in Brazilian commercial granites. *Radiat. Meas.* 39, 245–253.
- Baeza, A., Del Rio, M., Jimenez, A., Miró, C., Paniagua, J., (1995) : Influence of geology and soil particle size on the surface-area/volume activity ratio for natural radionuclides. *J. Radioanal. Nucl. Chem.* 189, 289–299.
- Boyle, R. W. (1982): *Geochemical prospecting for thorium and uranium deposits.* Elsevier Publ. Co., Amsterdam, 498 p.
- Brantley, S. L.; Kubicki, J. D. and White, A. F. (2008): *Kinetics of Water-Rock Interaction*, Springer Science-Business Media, LLC, New York, USA, pp. 833.
- Cathelineau, M., and Holliger, P., (1987): Polyphase metallogenesis of hydrothermal uranium veins from the southern Armorican massif, France. *Proc. Intern. Meet. Nancy, France*, 212-217.
- Cowart, J.B., Burnett, W.C., (1994): The distribution of uranium and thorium decay-series radionuclides in the environment. *J. Environ. Quality* 23, 651–662.
- De Jong, E., Acton, D.F., Kozak, L.M., (1994): Naturally occurring gamma-emitting isotopes, radon release and properties of parent materials of Saskatchewan soils. *Canad. J. Soil Sci.* 74, 47–53.
- El Feky M.G., El Mowafy A. A., and Abdel Warith A. (2011): Mineralogy, geochemistry, radioactivity and environmental impacts of Gabal Marwa granites, southeastern Sinai, Egypt. *Chin.J.Geochem.*, 30, 175–186.
- El-Galy, M. M., (1998): *Geology, radioactivity, geochemistry and tectonic setting of selected granitic rocks, West Gulf of Aqaba, Sinai, Egypt*, Ph.D Thesis, Tanta Univ., Egypt, 324p.
- El Nahas, H. A.; El Zalaky, M. A. and Abuseteet, A. A. (2011): Integrated remote sensing, GIS and stream sediments studies for the prediction of radioactive mineralizations around Wadi El Reddah, North Eastern Desert, Egypt.
- Hansink, J. D., (1976): Equilibrium analysis of sandstone rollfront uranium deposits. *Proceedings international symposium on exploration of uranium ore deposits*, IAEA, Vienna, 683-693p.
- Hussein, A. A., (1978): *Lecture course in nuclear geology*, NMA, Egypt, 101p.
- IAEA, 1979: International Atomic Energy Agency “Gamma-Ray Survey in Uranium Exploration” IAEA Technical Report Series, No. 186, Vienna, Austria, pp. 90.
- IAEA, 1987: *Preparation and Certification of IAEA Gamma Spectrometry Reference Materials, RGU-1, RGTh-1 and RGK-1.* International Atomic Energy Agency. Report-IAEA/RL/148.
- Killen, P.G., (1979): Gamma ray spectrometric methods in uranium exploration—application and interpretation; in *Geophysics and Geochemistry in the Search for Metallic Ores*; Hood, P.J., ed., Geol. Surv. Can., Economic Geology Report 31, p. 163-229.
- Marchenko, Z., (1986): *Spectrophotometric determination of elements.* John Wiley and Sons: Inc., New York, 540-542.
- Matoline, M. (1990): *A report to the government of the Arab Republic of Egypt. “Construction and use of spectrometric calibration pads”*, Egypt. Laboratory gamma-ray spectrometry.
- Megumi, K., Oka, T., Yaskawa, K., Sakanoue, M., (1982) : Contents of natural radioactive nuclides in relation to their surface area. *J. Geophys. Res.* 87, 10857–10860.
- Navas, A., Soto, J., and Machin, J., (2002): <sup>238</sup>U, <sup>226</sup>Ra, <sup>210</sup>Pb, <sup>232</sup>Th and <sup>40</sup>K activities in soil profiles of the Flysch sector ( Central Spanish Pyrenees). *Applied Radiation and Isotopes* 57 (2002) 579–589.
- Prikryl, J. D., Pickett D.A., Murphy, W. M., Pearcey E.C., (1997): Migration behavior of naturally occurring radionuclides at the Nopal I uranium deposit, Chihuahua, Mexico, *Journal of Contaminant Hydrology* 26, 61-69.
- Reeves, R.D. and Brooks, R.R., (1978): *Trace element analyses of geological materials.* John Wiley & sons Inc., New York, 421p.
- Remon, R. A., Emile, L.I. and Sayed, A.W. (2006): Stream sediments survey in Wadi Al Reddah, Gattar area, North Eastern Desert, Egypt. *Journal of the Faculty of Education*, 30, 117-141.
- Rosholt, J.N., Doe, B.R., Tatsumoto, M., (1966): Evolution of the isotopic composition of uranium and thorium in soil profiles. *Geol. Soc. Am. Bull.* 77, 987-1004.
- Sully, M.J., Flocchini, R.G., Nielson, D.R., (1987): (Linear distribution of naturally occurring radionuclides in a Mollic Xerofluvent. *Soil Sci. Soc. Am. J.* 51, 276-281.
- Surour, A.A., El-Bayoumi, R.M., Attawiya, M.Y. and El-Feky, M.G., (2001): *Geochemistry of wall rock alterations and radioactive mineralization in the vicinity of Hangaliya auriferous shear zone, Eastern Desert, Egypt.* *Egyptian Journal of Geology*, 45(1): 187-212.